Available online at www.sciencedirect.com
SCIENCE DIRECT®
Diamond and Related Materials 13 (2004) 590–594
DIAMOND AND RELATED MATERIALS
www.elsevier.com/locate/diamond

Characterization of diamond nanoplatelets

Hou-Guang Chen*, Li Chang

Department of Materials Science and Engineering, National Chiao Tung University, 1001 Ta Hsueh Road, Hsinchu, Taiwan 300, ROC

Abstract

Diamond deposition at a temperature above 1000 °C was carried out in a microwave plasma chemical vapor deposition reactor using a 3% CH_4/H_2 gas mixture. A polycrystalline diamond substrate was coated with a thin film of nickel in 100-nm thickness before deposition. Electron microscopy characterization of electron diffraction, high-resolution imaging, and electron energy loss spectroscopy shows that the diamonds deposited exhibit regular shapes in triangles and parallelogram with well-faceted surfaces. These diamond platelets are single crystallites with a uniform thickness of approximately 30–70 nm and length of several hundred nanometers to a few micrometers. The platelet morphology suggests that it is formed by lateral growth. Also, it was found that the diamonds are covered with a 1 to 2-nm thick graphite films in epitaxy.

Keywords: Nanodiamond; Transmission electron microscopy (TEM); Microstructure; Electron energy loss spectroscopy

1. Introduction

Synthesis of diamond has attracted intensive attention in the past decade, due to its excellent properties such as wide band gap, the high thermal conductivity, chemical inertness, the highest hardness and well biological compatibility [1,2]. Recently, the field of nanocrystalline materials which possess noticeable physical properties has been mostly focused. Simultaneously, the research on synthesis of nanocrystalline or nanostructured diamond has also received increasing attention, and many preparation methods have been reported, such as plasma discharge chemical vapor deposition method [3,4], pulsed laser-induced liquid–solid interfacial reaction method [5], plasma etching diamond substrate [6,7] and patterned aluminum oxide templates [8]. However, nanocrystalline diamond prepared by plasma-enhanced chemical vapor deposition process usually appear in irregular crystal shape or cauliflower-like in diamond films, which includes high defect densities such as fivefold twins, stacking faults, and grain boundaries [3,4,9,10] but nanodiamonds in well-defined shape with low defect densities are rarely reported. In fact, the preparation of well-defined single crystalline nanodiamond materials free of defects is important for diamond applications in nanotechnology.

In this paper, we show that a unique nanostructure of single-crystalline diamond can be successfully synthesized by microwave plasma chemical vapor deposition. The diamonds appeared as a nanosheet or platelet configuration with uniform thickness of several tens of nanometers and a flat well-faceted morphology. The result verifies that the synthesis of single-crystalline diamond in a specific nanostructure is feasible.

In order to characterize diamond platelet, scanning electron microscopy and transmission electron microscopy were employed to analyze microstructure of the platelets. The bonding structure and chemistry of diamond platelets were examined by electron energy loss spectroscopy with energy-filtering image technique.

2. Experimental

2.1. Synthesis of diamond platelets

Before the formation process, polycrystalline diamond substrates were prepared by hot-filament chemical vapor deposition on bare Si (100) wafers. Then, a 100-nm thick nickel film was coated on the poly-diamond substrate by electron beam evaporation. The synthesis of diamond platelets was carried out in a 2.45 GHz ASTeX microwave plasma CVD reactor. The sample

*Corresponding author. Tel.: +886-3-5712121x55373; fax: +886-3-5724727.
E-mail address: houguang.mse88g@nctu.edu.tw (H.-G. Chen).

0925-9635/04/$ - see front matter © 2003 Elsevier B.V. All rights reserved.
doi:10.1016/j.diamond.2003.11.013

was placed on the graphite disc. The substrate was heated to 850 °C as measured by an optical pyrometer by hydrogen plasma for 5 min at 800 W to allow for cleaning of the substrate surface. After heating, the growth process was performed by increasing microwave power to 1000 W and process pressure to approximately 60 Torr. The 3% CH_4 concentration in H_2 was used as source gas. The substrate temperature was above 1000 °C. Duration of the MPCVD process was approximately 2 h.

2.2. Characterization of diamond platelets

After deposition, the morphology was examined using a field-emission scanning electron microscope (SEM) (Hitachi S-4700 FEG at 15 kV). The specimens for transmission electron microscopy (TEM) analysis were prepared by dispersing diamond in methanol with ultrasonic treatment, followed by dipping on a holey carbon film supported on a copper grid. A Philips Tecnai 20 TEM was employed for TEM observation and selected-area diffraction (SAD) analyses. Electron energy-loss spectroscopy (EELS) was performed using a Gatan Imaging Filter equipped with the TEM. In the EELS analysis, we acquired spectra in diffraction mode with a semi-collection angle approximately $\sim$3.9 mrad.

3. Results and discussion

3.1. Morphology characterized by SEM and TEM

After deposition, observations of the surface morphology were performed by SEM. In Fig. 1a, the SEM image shows a large number of platelets with lengths of several hundred nanometers to a few micrometers. Some platelets stand perpendicularly on the substrate, so that side-view characteristics of these platelets exhibit long and thin morphology. Approximately 20–30 nm thickness of thin platelets can be observed from high-magnification SEM image, as shown in Fig. 1b, and the facets of each platelet can be clearly observed.

The diamond platelets were further characterized by TEM. A bright field TEM image in Fig. 1c reveals the typical configuration of platelets. The platelets exhibit regular shapes in triangles and parallelogram with well-faceted surfaces. The image contrast reveals the uniform thickness and low defect densities included. It also shows that each straight edge of diamond platelet is inclined with a specific angle, typically of 60 and 120°. The inset shows the corresponding selected area diffraction pattern which belongs to cubic diamond (space group Fd3 m, $a=0.3567$ nm) single crystal diffraction pattern in [111] zone-axis. According to the SAD, all the edges of diamond platelet are along ⟨110⟩ directions and the top and bottom surfaces are parallel to {111} plane. The side surfaces of diamond platelets might be

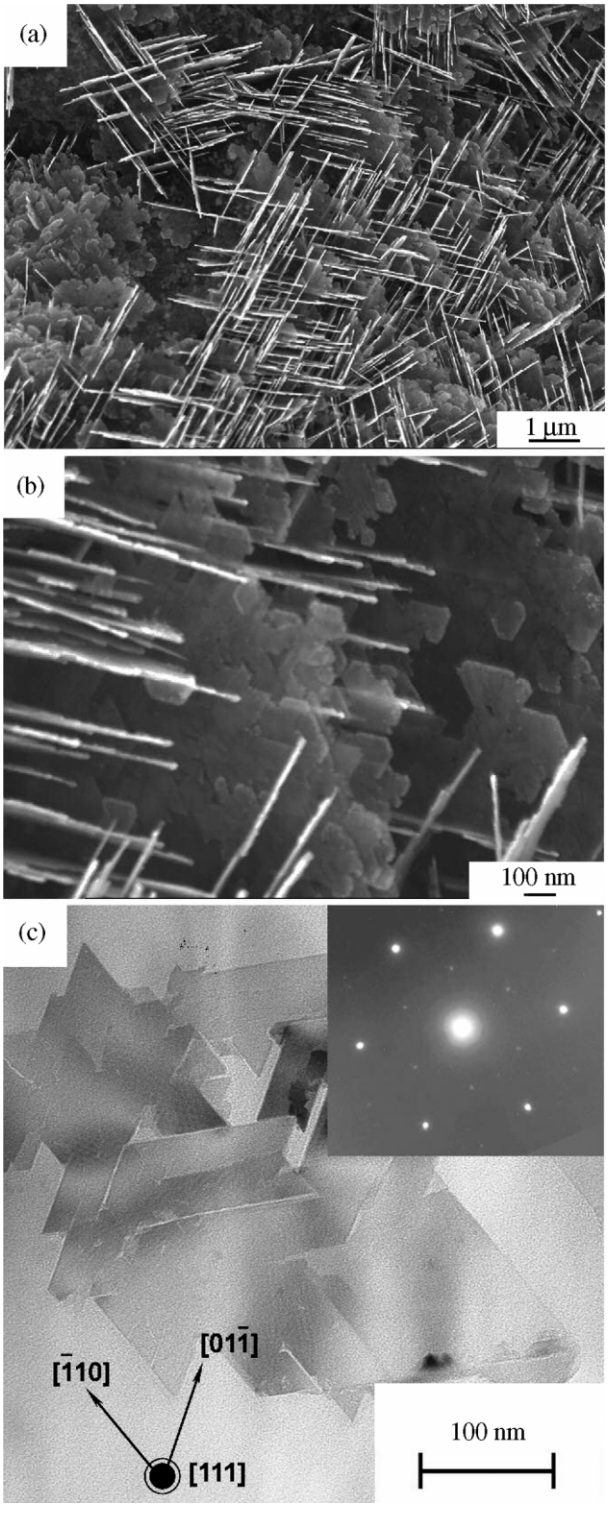

Fig. 1. (a) SEM micrograph of platelets; and (b) a magnified SEM micrograph showing that the thickness of platelets was approximately 30 nm. (c) TEM micrograph showing diamond platelets with well-faceted morphology; the inset showing electron diffraction pattern of the platelet corresponding to diamond diffraction pattern in [111] zone axis.

parallel to {112} which were commonly observed as lateral step of facets on diamond {111} surface in homoepitaxial growth [11]. In addition to diamond diffraction spots, we also find an extra set of very weak diffraction spots with six-fold symmetry in the SAD patterns. The lattice spacing of the weak diffraction spots is approximately 0.216 nm, which could be indexed as graphite (space group $P6_3/mmc$, $a=0.247$ nm, $c=0.693$ nm) 1010 reflection (0.213 nm). However, such positions are also close to 1/3{422} reflections of diamond (0.217 nm), as usually observed in thin fcc crystals with atomically flat surface [12,13]. Thus, the weak diffraction spots were probably contributed from both cases.

3.2. Characterization of graphite on diamond platelets

In Fig. 2a, it shows the bright-field image of another piece of diamond platelet. In addition to the similar morphology shown in Fig. 1c, Moiré fringes can be clearly observed on the platelets, resulting from interference of two overlapped crystals with close periodicity. Fig. 2b is the enlargement of Fig. 2a, showing that the crossed fringes have an angle near 60° and the spacing of the fringe is approximately 57.6 Å. According to SAD, these fringes relate to the diffraction spots of diamond 220 and the graphite 1120, which have small difference in interplanar spacings (approx. 0.02 Å). Theoretical calculation of Moiré fringe spacings between diamond {022} and graphite {1120} is approximately 54.7 Å that is close to the measured values within experimental error at the operation magnification. The results of diffraction patterns and Moiré fringes show that the crystallographic relationship of the graphite with the diamond is $\langle 111\rangle_{dia}//\langle 0001\rangle_{graphite}$ and $\{110\}_{dia}//\{1210\}_{graphite}$, suggesting a graphite layer would epitaxially cover the surfaces of diamond platelets. In order to further realize the detailed structure of graphite layer on diamond platelets, HRTEM was employed. Fig. 2c shows a HRTEM image of a side face of a diamond platelet. Diamond {111} lattice fringes (fringe spacing of 0.206 nm) and fringes of graphite {0002} plane (fringe spacing of 0.346 nm) can be clearly seen. From the image, it is shown that the diamond platelet is actually sheathed by an ultra-thin graphite layer (approx. 1–2 nm). It is possible that plasma etching of diamond surface or high deposition temperature (>1000 °C) would induce partially graphitization of the diamond on the surface [14].

3.3. Electron energy loss spectroscopy and energy-filtering image characterization of diamond platelets

EELS was also used to characterize the diamond platelets. The chemical bonding state of diamond platelets can be easily distinguished by EELS technique. Fig.

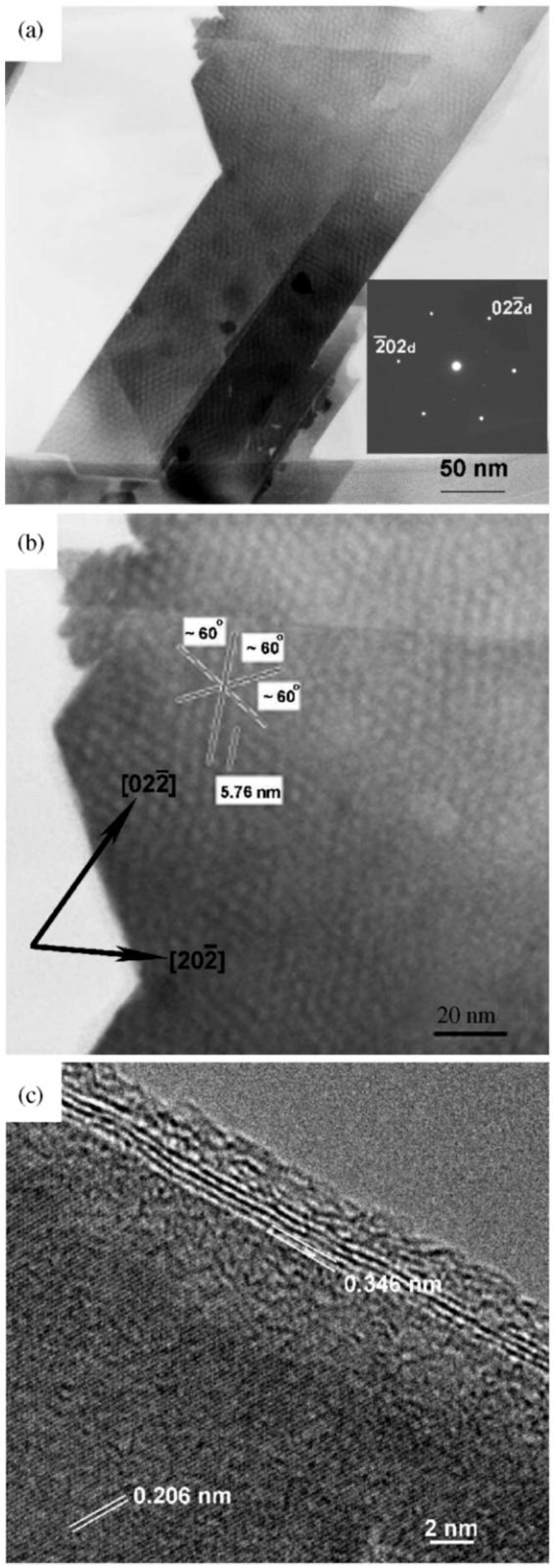

Fig. 2. (a) TEM micrograph showing the diamond platelets; the inset showing the diffraction pattern; and (b) enlargement in Fig. 2a showing Moiré fringes. (c) HRTEM micrograph from another platelet revealing a graphite layer covering on diamond platelet surface.

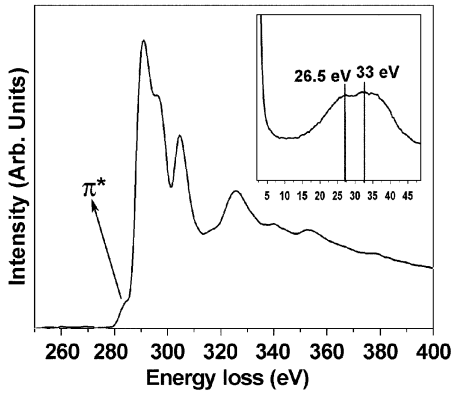

Fig. 3. EELS spectrum of diamond platelet showing carbon K edge; and the inset showing the low energy loss region.

3 reveals the near edge structure of carbon K-edge from a platelet. The K-edge shape of carbon has predominantly the characteristics of diamond in addition of a small peak at 285 eV corresponding to the π^* orbit of sp^2 carbon as a result of the graphite sheath on diamond platelets. The results of EELS study are in excellent agreement with the interpretation of TEM image and electron diffraction that diamond is the major component in the platelets. Inset in Fig. 3 is low energy loss region of the spectrum. The low energy loss region shows the plasmon peaks at 26.5 and 33 eV, which are near those of the graphite (27 eV) and natural diamond (33 eV), respectively [15]. The information of specimen thickness can be estimated by log-ratio method from the low-loss region. In this spectrum, the thickness of the platelets is approximately 34 nm. The estimated thickness by EELS is within the range of measured by SEM images.

The thickness-map image could also be obtained by log-ratio calculation from the unfiltered image and the zero energy loss image. Using the equation

$$\frac{t}{\lambda} = \ln\left(\frac{I_u}{I_0}\right) \tag{1}$$

where I_u is unfiltered image intensity and I_0 is zero energy loss intensity. Then, we can obtain a thickness map in units of relative thickness (t/λ), where λ is an effective mean free path and t is an absolute thickness of sample. Based on the thickness map, the variation of thickness across the sample can be revealed, so that the three-dimension contours of diamond platelet could clearly be described. Fig. 4a,b are the unfiltered image and the elastic image of diamond platelet, respectively. In thickness-map image (Fig. 4c) the area with stronger image contrast has thicker thickness. The image indicates that the surface has terrace structure, and several sharp steps with straight edge on the diamond platelet can also be found. As shown in Fig. 4d, line profiles I and II of thickness across the steps of the same terrace are revealed the same step height of approximately $0.05t/\lambda$. Therefore, it is believed that each terrace is of

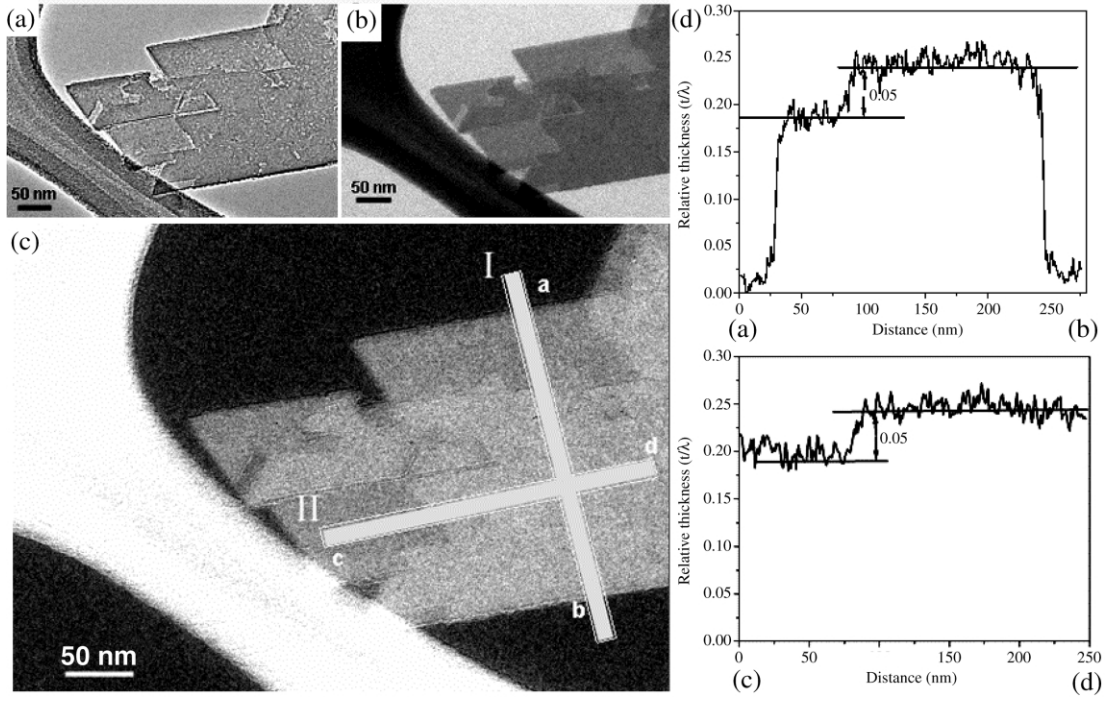

Fig. 4. (a) Unfilter image, (b) zero energy loss image, and (c) thickness map from diamond platelets. (d) Thickness profiles taking from I and II line in Fig. 4c, respectively.

uniform thickness. The growth of diamond platelets is likely to proceed as layer-by-layer growth in lateral directions.

The elemental analyses of diamond platelet by X-ray energy dispersive spectroscopy (EDS) and EELS show no detection of any Ni, implying that Ni atom are not included in the diamond platelets. The influence of Ni on formation of diamond nanoplatelets is still unknown which will be clarified in future work.

4. Conclusion

Single crystalline diamond nanoplatelets with low defect densities have been achieved on Ni-coated polycrystalline diamond substrate by MPCVD process. Electron diffraction verifies that the platelets are single crystalline. The morphologies of the diamond nanoplatelets revealed by SEM and TEM have regular shapes in triangles and parallelogram with well-faceted surfaces and with a uniform thickness approximately ranged from 30 to 70 nm. The edges of platelets are along ⟨110⟩ directions with top and bottom surfaces parallel to {111} planes. The EELS spectra show the diamond is the major component in the platelets. The thickness mapping indicates that the surfaces consist of terrace structure. The platelet morphology suggests that it is formed by lateral growth. Observation of ultra-thin graphite layers eptaxially sheathing diamond platelet surfaces is demonstrated by Moiré fringes, HRTEM and EELS.

Acknowledgments

This work was supported by the National Science Council, Taiwan, ROC, under contract of NSC 91-2216-E-009-014 and NSC 92-2116-E-009-011.

References

[1] I. Jan, H. Johan, J. Erik, W. Tobias, J.T. Daniel, J.W. Andrew, et al., Science 297 (2002) 1670.
[2] W.S. Yang, O. Auciello, J.E. Butler, W. Cai, J.A. Carlisle, J. Gerbi, et al., Nat. Mater. 1 (2002) 253.
[3] X. Jiang, C.L. Jia, Appl. Phys. Lett. 80 (2002) 2269.
[4] X.T. Zhou, Q. Li, F.Y. Meng, I. Bello, C.S. Lee, S.T. Lee, et al., Appl. Phys. Lett. 80 (2002) 3307.
[5] L.B. Wang, C.Y. Zhang, X.L. Zhong, G.W. Yang, Chem. Phys. Lett. 361 (2002) 86.
[6] K. Kobashi, T. Tachibana, Y. Yokota, N. Kawakami, K. Hayashi, K. Inoue, Diamond Relat. Mater. 10 (2001) 2039.
[7] E.S. Baik, Y.J. Baik, S.W. Lee, D. Jeon, Thin Solid Films 377–378 (2000) 295.
[8] H. Masuda, T. Yanagishita, K. Yasui, K. Nishio, I. Yagi, T.N. Rao, et al., Adv. Mater. 13 (2001) 247.
[9] D. Shechtman, A. Feldman, M.D. Vaudin, J.L. Hutchison, Appl. Phys. Lett. 62 (1993) 487.
[10] D. Dorignac, V. Serin, S. Delclos, F. Phillipp, D. Rats, L. Vandenbulcke, Diamond Relat. Mater. 6 (1997) 758.
[11] T. Tsuno, T. Tomikawa, S. Shikata, N. Fujimori, J. Appl. Phys. 75 (1994) 1526.
[12] R.C. Jin, Y.W. Cao, C.A. Mirkin, K.L. Kelly, G.C. Schatz, J.G. Zheng, Science 294 (2001) 1901.
[13] M. Maillard, S. Griorgio, M.P. Pileni, Adv. Mater. 14 (2002) 1084.
[14] G. Jungnickel, D. Porezag, T. Frauenheim, M.I. Heggie, W.R.L. Lambrecht, B. Segall, et al., Phys. Status Solidi A 154 (1996) 109.
[15] A. Duarte-Moller, F. Espinosa-Magaña, R. Martinez-Sanchez, M. Avalos-Borja, G.A. Hirata, L. Cota-Araiza, J. Electron Spectrosc. 104 (1999) 61.